High-Pressure Studies of Pharmaceuticals: An Exploration of the Behavior of Piracetam

8 AUTHORS, INCLUDING:

David R Allan
Diamond Light Source
84 PUBLICATIONS **2,249** CITATIONS

SEE PROFILE

Simon Parsons
The University of Edinburgh
448 PUBLICATIONS **13,119** CITATIONS

SEE PROFILE

Colin Pulham
The University of Edinburgh
140 PUBLICATIONS **2,310** CITATIONS

SEE PROFILE

John Edward Warren
The University of Manchester
175 PUBLICATIONS **3,964** CITATIONS

SEE PROFILE

High-Pressure Studies of Pharmaceuticals: An Exploration of the Behavior of Piracetam

Francesca P. A. Fabbiani,*,† David R. Allan,† William I. F. David,‡ Alistair J. Davidson,†
Alistair R. Lennie,§ Simon Parsons,† Colin R. Pulham,† and John E. Warren§

*School of Chemistry and Centre for Science at Extreme Conditions, The University of Edinburgh,
King's Buildings, West Mains Road, Edinburgh, EH9 3JJ, UK, ISIS Neutron Facility, Rutherford
Appleton Laboratory, Chilton, Didcot, OX11 0QX, UK, and CCLRC Daresbury Laboratory,
Warrington, WA4 4AD, UK*

ABSTRACT: The structural response of the nootropic drug piracetam (2-oxo-pyrrolidineacetamide) to both direct compression and high-pressure recrystallization from aqueous solution is reported. Crystals obtained by these methods have been characterized in situ by single-crystal X-ray diffraction. Compression of form II between pressures of 0.45−0.70 GPa caused a reversible, single-crystal to single-crystal transition to give a new polymorph, form V. Crystallization from a dilute aqueous solution of piracetam at a pressure of 0.6 GPa via crystallization of high-pressure ice-VI resulted in the formation of a previously unreported dihydrate. The molecular packing arrangements of these new structures are compared with the known polymorphs and hydrates of piracetam. This study highlights how the systematic variation of pressure is a powerful method for the exploration of polymorphism and solvate formation and has the potential to add a further dimension to polymorph screening of pharmaceuticals.

Introduction

The importance of polymorphism and solvate formation in the crystallization of organic compounds is widely recognized within the industrial and academic communities.[1] Within the pharmaceutical industry, the identification of polymorphic forms of drug compounds is of crucial importance. Polymorphs, hydrates, and solvates can be produced by a variety of standard pharmaceutical processes.[2] Two polymorphs of the same drug compound may have very different physical properties that affect bioavailability or processibility (e.g., tabletting),[3] and drug regulatory authorities demand detailed information about polymorphism before granting licenses for product distribution. Intellectual property can also become an issue for the pharmaceutical companies who develop and market new drug products, where challenges to patents have been made on the basis of the discovery of a new polymorph. The search for polymorphs is therefore an area of intense activity. Pharmaceutical companies deploy substantial effort and resources for the identification and characterization of polymorphs and solvates. These techniques typically involve recrystallization—increasingly via high-throughput robotic screening—by varying parameters such as temperature, concentration, solvent, and relative humidity, with subsequent analysis by calorimetric, spectroscopic, and diffraction techniques.[4] Almost all recrystallization studies in the pharmaceutical industry that seek to systematically screen for polymorphism and solvate formation are performed under ambient pressure. The only exceptions are a few processes that use supercritical fluids—such as carbon dioxide—as solvents, but the pressures rarely exceed 0.01 GPa and the pressure ranges are narrow.[5] Furthermore, the range of easily accessible supercritical solvent systems is limited to only a small number of solvents. Of more long-standing and growing interest is the
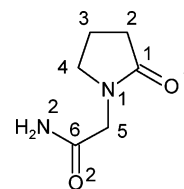
Figure 1. Molecular structure of piracetam with numbering scheme.

effect of pressure on solid drugs during processing, since many solid drugs are subjected to mechanical action during various stages of drug manufacturing.[6,7] Typical processes include milling and grinding, both of which can cause localized increases in pressure and shear stress that can on occasion induce phase transitions.[8] The first high-pressure compression studies of pharmaceuticals date back to Bridgman.[9,10] More recently, a study of indomethacin has reported, using slurry techniques, how the relative stability of a polymorph can be modified by pressures up to 0.4 GPa.[11] This study also illustrated the importance of the solvent in mediating phase transitions since compression of γ-indomethacin in the absence of solvent did not result in a phase transition. The effects of pressure-transmitting fluids on pressure-induced transitions was also described for [Co(NH₃)₅NO₂]I₂.[12] Of notice are also the detailed compression studies of the polymorphs of paracetamol and fenacetine at hydrostatic conditions to 4.0 GPa[13] and of chlorpropamide A at quasihydrostatic pressure to 5.5. GPa.[14]

It is well-known that the application of pressure to a wide range of materials (e.g., metals, alloys, minerals, and ices) is a very effective method for inducing phase transitions. Recent studies have demonstrated that high pressure is also effective at inducing phase transitions in a range of organic compounds such as alcohols, cyclic β-diketoalkanes, carboxylic acids, and amino acids.[15−18] Comparative studies of different polymorphs of the same compound can provide a better understanding of intermolecular interactions. These interactions are important in understanding some of the properties of solid drugs, including crystallization, dissolution, and bioavailability, as well as for improving potentials used for structure and polymorph predic-

* To whom the correspondence should be addressed. Present address: CCLRC Rutherford Appleton Laboratory, R3 2-24, Fermi Avenue, Chilton, OX11 0QX, UK. Tel: +44 (0)1235 445 137. Fax: +44 (0)1235 445 720. E-mail: Francescapaola@gmail.com.
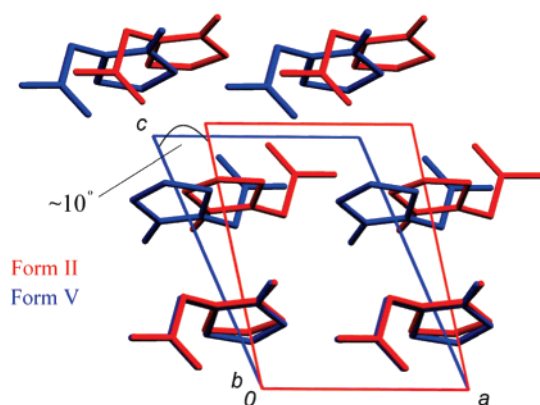† University of Edinburgh.
‡ Rutherford Appleton Laboratory.
§ CCLRC Daresbury Laboratory.
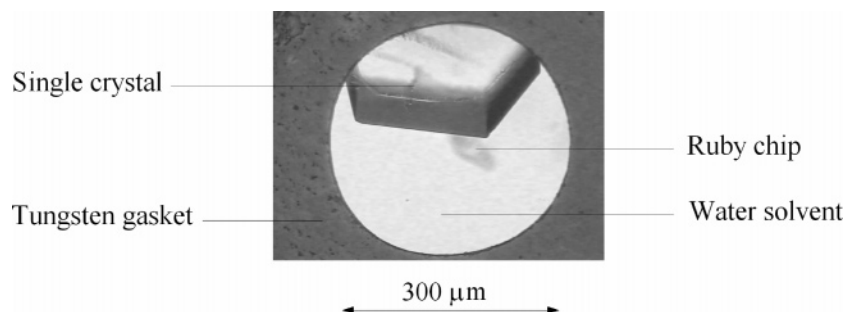
Figure 2. Optical image of a single crystal of piracetam dihydrate at 0.6 GPa in a DAC.

Figure 3. Overlay of form II at 0.45 GPa and form V at 0.7 GPa.

tions. The effects of pressure on molecular crystals have been recently reviewed in the literature.[19−21]

Pressure-induced freezing of a liquid[9,10,15,22] is a very powerful method for accessing new polymorphs from compounds with relatively low melting points;[15,23,24] however, it is less applicable to compounds such as pharmaceuticals that typically have melting points significantly higher than ambient temperature. The problem is made more difficult by the substantial increase in melting point induced in most substances by the application of pressure. Generally, decomposition or some undesirable chemical reaction takes place before the compound melts.

We recently described an approach that overcomes these problems and is tailored for the study of polymorph and solvate formation of compounds that have melting points significantly higher than ambient temperature. Using the technique of high-pressure recrystallization from solution, we prepared and characterized new polymorphs of phenanthrene,[25] pyrene,[26] and acetamide[27] and new solvates of paracetamol[25,28] and parabanic acid.[27] The technique involves loading a diamond-anvil cell (DAC) with a solution of the compound of interest and growing a single crystal by temperature cycling of polycrystalline material that precipitates from solution in situ in the DAC as a result of the application of pressure. This technique is particularly suited for studying the polymorphism of high-melting compounds (e.g., pharmaceuticals), where thermal decomposition of the compound usually occurs long before the pressure-enhanced melting temperature is reached or for which the substantial kinetic barrier to molecular rearrangement involved in a polymorphic transition cannot be overcome by direct compression. Furthermore, the technique also allows the effects of different solvent systems to be studied, thereby providing opportunities for preparing new solvates.

Piracetam (2-oxo-pyrrolidineacetamide) is a nootropic agent, currently marketed by UCB Pharma as Nootropil, that is used to treat conditions of age-associated mental decline and disorders

of the nervous system (see Figure 1 for the molecular structure). Although a rather simple molecule, it represents an ideal candidate for study since it contains two different amide groups and possesses conformational flexibility. Three polymorphs of piracetam have been identified and structurally characterized. Forms II (triclinic, $P\bar{1}$) and III (monoclinic, $P2_1/n$) can be prepared by recrystallization from various solvents (e.g., methanol, propan-2-ol) under ambient conditions, and crystal structures for both forms have been reported.[29,30] Both forms transform above 400 K into the high-temperature phase denoted as form I (triclinic, $P\bar{1}$). This can be recovered to ambient temperature by quenching but transforms within a few hours at 298 K into form II. Its crystal structure has been determined from X-ray powder diffraction in combination with minimization of the crystal-lattice potential energy[31] and more recently by single-crystal X-ray diffraction.[32]

All three polymorphs have been studied by thermochemical methods and shown to be enantiotropically related.[33−35] The hierarchical stability of these polymorphs was studied by relating sublimation vapor pressures to measurements made by differential scanning calorimetry.[33] These studies concluded that at ambient temperatures the stability order is II > III > I, while above 399 K the stability order is I > II > III.[33] However, these results are in disagreement with those obtained from studies using thermomicroscopy and DSC measurements, which showed that at ambient temperature form III is more stable than form II.[34]

The III → I phase change has also been studied at high pressure. After compression of a sample of form III to ca. 0.2 GPa at 443 K followed by decompression, the III → I transition was recorded at 0.156 GPa.[36] Form III has been identified as the stable form at higher pressures on the basis of these observations and because it is the densest of the three forms under ambient conditions.[33] Lattice energy calculations using the atom−atom potential method[37] have been performed to give values of −87.29, −97.30, and −99.44 kJ mol^{-1} for phases I, III, and II, respectively.[31] These calculations also located another distinct minimum at −100.78 kJ mol^{-1}, but this structure has never been observed experimentally. Three further polymorphs have been postulated on the basis of morphological changes and differences in optical polarization observed on cooling from the melt, but in all cases transformation into form II occurred very rapidly at room temperature.[34]

It was recently demonstrated how the systematic variation of pressure, in combination with studies at ambient pressure, could be used not only to identify rapidly all of the known polymorphs of the nootropic drug piracetam but also to identify and characterize new polymorphs and hydrates.[32] This previous study stemmed from the intriguing observation that although piracetam has been extensively studied in a range of solvents, no hydrates or other solvates had been previously reported in

Table 1. Crystal, Collection, and Refinement Details for All Compounds

	Form II 0.45 GPa	Form V 0.7 GPa	Form V 0.9 GPa	Form V 2.5 GPa	Form V 4.0 GPa	dihydrate 0.6 GPa
chemical formula	$C_6H_{10}N_2O_2$	$C_6H_{10}N_2O_2$	$C_6H_{10}N_2O_2$	$C_6H_{10}N_2O_2$	$C_6H_{10}N_2O_2$	$C_6H_{10}N_2O_2 \cdot 2(H_2O)$
M_r	142.16	142.16	142.16	142.16	142.16	178.19
crystal system, space group	triclinic, $P\bar{1}$	triclinic, $P\bar{1}$	triclinic, $P\bar{1}$	triclinic, $P\bar{1}$	triclinic, $P\bar{1}$	triclinic, $P\bar{1}$
a, b, c (Å)	6.321 (2), 6.5597 (11), 8.380 (4)	6.442 (2), 6.3530 (11), 8.737 (3)	6.3903 (7), 6.2932 (11), 8.6450 (16)	6.263 (2), 6.2063 (10), 8.412 (3)	6.169 (2), 6.1602 (11), 8.287 (3)	6.217 (2), 7.0356 (9), 10.0593 (13)
α, β, γ (°)	79.82 (3), 102.34 (3), 90.94 (2)	81.43 (3), 112.88 (2), 91.38 (2)	81.106 (12), 113.680 (12), 91.295 (11)	80.77 (3), 114.69 (2), 91.12 (2)	80.41 (3), 115.33 (3), 91.15 (2)	84.711 (12), 76.83 (2), 75.77 (2)
V (Å³)	334.0 (2)	325.53 (17)	314.26 (9)	292.81 (17)	280.23 (17)	414.98 (16)
Z	2	2	2	2	2	2
D_x (Mg m⁻³)	1.413	1.450	1.502	1.612	1.685	1.426
temperature (K)	293 (2)	293 (2)	293 (2)	293 (2)	293 (2)	293 (2)
no. of measured, independent and observed ($I > 2\sigma(I)$ reflections	1016, 363, 222	1013, 356, 226	2136, 423, 332	945, 332, 257	859, 317, 221	5183, 611, 493
R_{int}	0.0712	0.0811	0.039	0.0550	0.0696	0.047
θ_{max} (°)	25.0	24.8	25.1	25.0	24.9	25.1
completeness (%)	26.7	27.4	32.8	27.7	28.1	35.9
$R[F^2 > 2\sigma(F^2)]$, $wR(F^2)$, S	0.115, 0.300, 1.06	0.088, 0.230, 1.05	0.080, 0.207, 1.06	0.086, 0.214, 1.06	0.091, 0.240, 1.06	0.035, 0.091, 1.06
no. of reflections	323	332	411	321	292	608
no. of parameters	41	41	41	41	41	127
no. of restraints	23	23	23	23	23	89
H-atom treatment	constrained	constrained	constrained	constrained	constrained	mixture of independent and constrained refinement

Table 2. Crystallographic Data for Polymorphs and Hydrates of Piracetam

	Form[a]	Form II[b]	Form III[b]	Form IV 0.4 GPa[a]	Form V 0.7 GPa[c]	monohydrate	dihydrate 0.6 GPa[c]
CSD reference code	BISMEV05	BISMEV	BISMEV01	BISMEV04		YAKVAJ	
crystal system	monoclinic	triclinic	monoclinic	monoclinic	triclinic	triclinic	triclinic
space group	$P2_1/n$	$P\bar{1}$	$P2_1/n$	$P2_1/c$	$P\bar{1}$	$P\bar{1}$	$P\bar{1}$
a/Å	6.7250(2)	6.403(3)	6.525(2)	8.9537(11)	6.442(2)	6.9376(2)	6.217(2)
b/Å	13.2570(4)	6.618(4)	6.440(2)	5.4541(6)	6.3530(11)	7.4450(2)	7.0356(9)
c/Å	8.0530(2)	8.556(6)	16.463(5)	13.610(4)	8.737(3))	9.1267(2)	10.0593(13)
α/°	90.0	79.85(3)	90.0	90.0	81.43(3)	97.732 (2)	84.71 (12)
β/°	98.603(2)	102.39(3)	92.19(3)	104.93(2)	112.88(2)	103.958 (2)	76.83(2)
γ/°	90.0	91.09(3)	90.0	90.0	91.38(2)	115.766 (2)	75.77(2)
V/Å³	709.87(4)	348.5(4)	691.3(4)	642.2(2)	325.53 (17)	396.24(2)	414.98 (16)
Z	4	2	4	4	2	2	2
D_c/g cm⁻³	1.330	1.355	1.366	1.470	1.450	1.342	1.426
T/K	150(2)	283−303	283−303	293(2)	293(2)	150(2)	293(2)

[a] Ref 32. [b] Ref 30. [c] This work.

the open literature. Hence, high-pressure recrystallization of aqueous and methanolic solutions of piracetam contained in a DAC at pressures of 0.07−0.40 GPa resulted in the formation of a new high-pressure polymorph of piracetam, form IV that was structurally characterized by single-crystal X-ray diffraction.[32] The discovery and characterization of the new form IV of piracetam also provided an excellent opportunity to test recent developments in crystal structure prediction, and through a systematic exploration of conformational space, a "blind" study successfully identified form IV as the most favorable computed crystal structure.[38]

Depressurization of form IV to ambient pressure resulted in the formation of form II via a single-crystal to single-crystal transition. Ambient pressure crystallization of piracetam from water gave a new monohydrate of piracetam, irrespective of concentration. More recently, a 1:1 cocrystal of piracetam and gentisic acid (*p*-hydroxybenzoic acid) has been obtained by recrystallization at ambient pressure.[39]

The aim of the present investigation was to extend the scope of high-pressure studies on piracetam to explore not only a wider range of crystallization conditions (e.g., concentration, pressure, temperature) but also the effects of direct compression on this material composed of molecules with significant conformational flexibility.

Experimental Section

General Procedures. The Merrill-Bassett DAC used in this study had a half-cell opening angle of 40°[40] and was equipped with 800 μm culet diamonds and tungsten gaskets with a 300 μm hole. A small piece of ruby was loaded in the DAC along each sample as a pressure calibrant. The pressure within the gasket hole of was determined by the ruby fluorescence method on excitation with a 532 nm, 10 mW diode laser.[41] The ruby fluorescence was dispersed and detected by a BETSA PRL spectrometer, with a measurement precision of ±0.05 GPa.

Compressions Studies of Form II. Initial experiments focused on direct compression of a single crystal of form II under hydrostatic conditions. Rather to our surprise, it proved unusually difficult to load the DAC with a suitable single crystal of form II. Single crystals of form II were grown at ambient pressure by slow evaporation of saturated solutions of piracetam (Sigma-Aldrich) in either 2-propanol or 1,4-
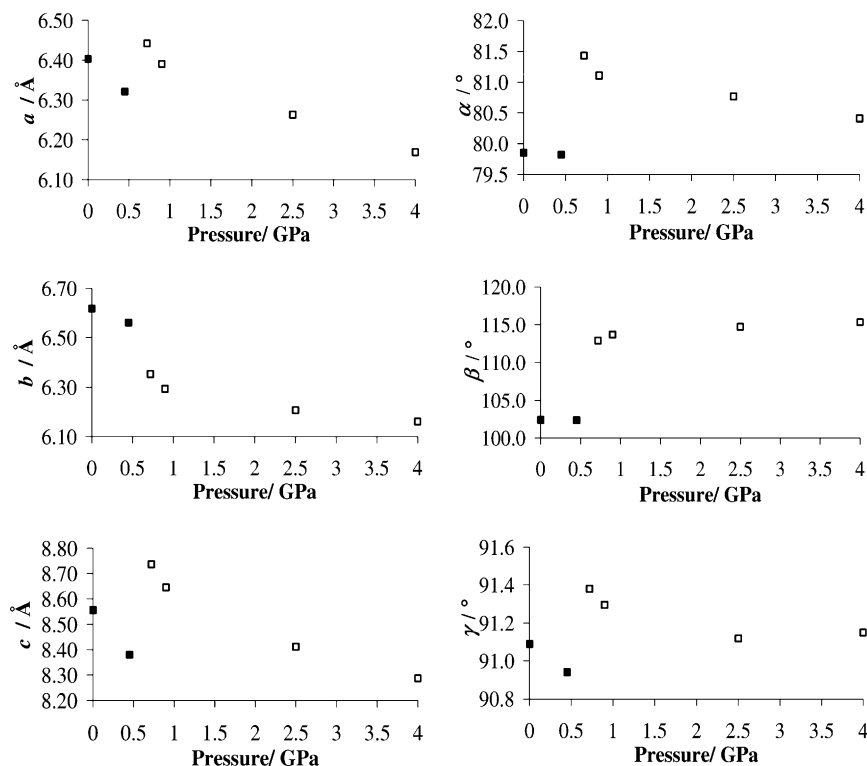
Figure 4. Variation of unit-cell parameters of forms II (filled symbols) and V (open symbols) as a function of pressure. The standard deviations are smaller than the plotted symbols.
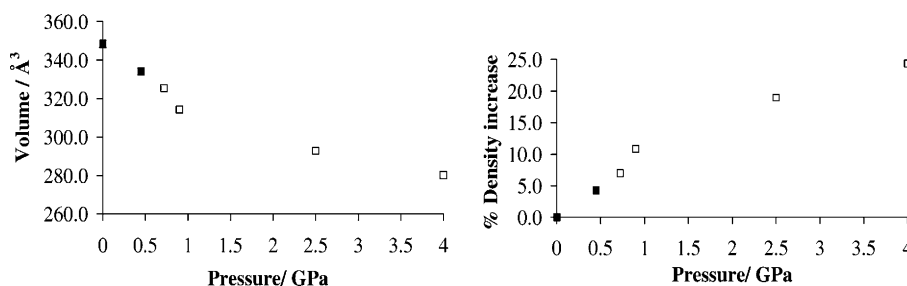
Figure 5. Variation of unit-cell volume and density of forms II (filled symbols) and V (open symbols) as a function of pressure. The standard deviations are smaller than the plotted symbols.

dioxane and were checked by determination of the unit-cell parameters. All attempts to cleave the crystals to the required size for loading resulted in damage, as confirmed by visual inspection with an optical microscope (the crystals exhibited shear damage irrespective of the direction of cleavage), or by checking the quality of the X-ray diffraction pattern (cleaved crystals did not diffract using either laboratory or synchrotron sources).

Attempts to grow a suitable single crystal of form II from 2-propanol at 0.2 GPa in the DAC also proved problematic. Seeding with small crystallites of form II (obtained from cleaving larger crystals) invariably resulted in crystallization of form III. This suggests that either cleavage of form II resulted in transformation to form III and that the transition is accompanied by damage of the single crystal, as confirmed by optical microscopy and by the absence of single-crystal diffraction of the cleaved crystal, or that form III is more stable at high pressure and hence crystallized preferentially. Evidence in support of the latter explanation has been provided by Toscani in a thermochemical study of piracetam.[20] Compression studies of powder samples of form II will be the subject of a future investigation. A single crystal of form II was finally grown by loading a DAC with a saturated solution (at 293 K) of piracetam and 2-propanol together with a few small crystallites (obtained by cutting larger crystals, as previously) of form II. The cell was sealed under a very minimum of pressure, such that a small air bubble remained visible in the gasket. The cell was then heated to ca. 313 K to dissolve all of the solid and then pressurized while warm to ca. 0.1 GPa. This ensured complete dissolution of all initial crystallites,

thus preventing nucleation of form III from possible crystal seeds present in the DAC. On cooling of the sample to 293 K, precipitation of small crystallites occurred. The temperature was then cycled near ca. 313 K to dissolve all but one of the crystallites and on slow cooling to 293 K a single crystal (colorless block, 0.20 × 0.15 × 0.15 mm) grew from solution to fill ca. 50% of the gasket hole. The cell was then pressurized to ca. 0.9 GPa. Indexing of the reflections gave a triclinic unit cell with reduced cell dimensions related to those of form II but with a significant increase of ca. 10° in the β angle, thereby suggesting a single-crystal to single-crystal transition to a new polymorph had occurred. This new form has been denoted as form V. The pressure inside the cell was subsequently decreased to 0.45 GPa, and indexing of reflections indicated the presence of form II: a dataset was collected at this pressure. The pressure inside the cell was then increased to ca. 0.7 GPa, and form V was again observed. Two further datasets in this compression study were subsequently collected at 2.5 and 4.0 GPa.

High-Pressure Recrystallization: Piracetam Dihydrate. A ca. 0.7 M aqueous solution of piracetam (Sigma-Aldrich) was loaded at 293 K into a DAC; the cell was sealed and pressurized in incremental steps, but no precipitation of polycrystalline material was observed up to pressures of 1.0 GPa. The cell was subsequently pressurized to 1.6 GPa to induce the crystallization of the aqueous solvent. The cell was depressurized in incremental steps and at 0.6 GPa ice crystals were observed to melt under a microscope, revealing the presence of finely divided powder. The temperature was then cycled near ca. 303 K to
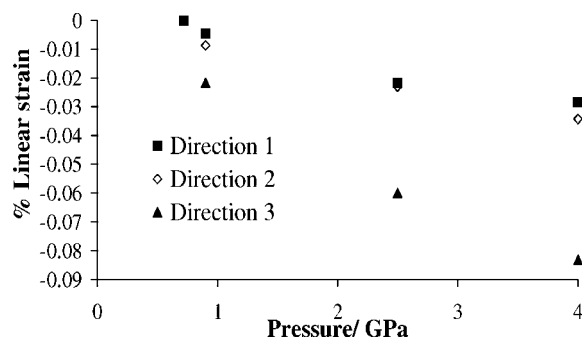
Figure 6. Plot of linear strain in the directions of the principal axes of strain ellipsoids vs pressure for piracetam-V. Directions: 1, minimum compression; 2, medium compression; 3, maximum compression.

dissolve all but one of the crystallites, and on slow cooling to 293 K a single-crystal grew (colorless block, $0.20 \times 0.15 \times 0.15$ mm) from solution to fill ca. 40% of the gasket hole (Figure 2).

X-ray Crystallography. All diffraction data were collected at Station 9.8 at the CCLRC Daresbury Laboratory, UK, with a Bruker APEX 2 CCD diffractometer at 293(2) K using synchrotron radiation ($\lambda = 0.6765$ Å). Data collection was performed according to an established 1-s ω-scans procedure.[42] Single-crystal diffraction data for piracetam dihydrate and form V at 0.9 GPa were collected with the DAC in three and two orientations, respectively (glued onto the goniometer head on three or two different sides of the cell), to simulate three different values of χ to improve data completeness. The strategy of collecting data with the DAC in two orientations for form V resulted in only a poor improvement of the overall data completeness (ca. 33% to $\theta_{max} = 25°$).

All single-crystal data were processed according to the procedure described by Dawson et al.[43] Data integration and global-cell refinement were performed using the program *SAINT*[43] in conjunction with dynamic masks.[43] Absorption corrections were then applied in a two-stage procedure with the programs *SHADE*[45] and *SADABS*.[46] Data were subsequently merged using the program *SORTAV*,[47] as incorporated in the *WinGX* suite.[48]

Structural refinement of form II at 0.45 GPa was carried out starting from the published coordinates determined at ambient pressure (CSD reference code BISMEV).[30] The structures of form V and piracetam dihydrate were solved by direct methods using *SIR92*.[49] Full-matrix least-squares structure refinement against $|F|^2$ was performed using *CRYSTALS*.[50] For forms II and V, all non-hydrogen atoms were refined isotropically owing to the low completeness of the datasets and primary bond distances and angles were restrained to the values observed in form II at ambient pressure; all hydrogen atoms were placed in calculated positions and fixed during refinement. In the case of piracetam dihydrate, all non-hydrogen atoms were refined anisotropically and rigid-bond and thermal similarity restraints were employed to obtain a satisfactory model. Hydrogen atoms involved in hydrogen bonding were located on a difference Fourier map and refined subject to distance restraints. A final *R*-factor of 3.5% was obtained, which represents an excellent refinement result of high-pressure data collected for a triclinic crystal system and allows reliable comparison with the structural features of the known anhydrous and monohydrate forms.

Some data collection and refinement statistics are given in Table 1, and the remainders are available in the CIFs deposited in Supporting Information.

Software and Other General Procedures. The structures were visualized using the programs *MERCURY*[50] and *DIAMOND*.[52]

Results and Discussion

Unit-cell parameters for the polymorphs and hydrates of piracetam are summarized in Table 2.

Compression Studies of Form II: The Transition to Form V. The direct transformation of form II to form V on application of pressure at ambient temperature is an interesting result because such pressure-mediated single-crystal to single-crystal transformations that proceed without destruction of the crystal are rare[17−20,53−59] and usually require the molecules to have
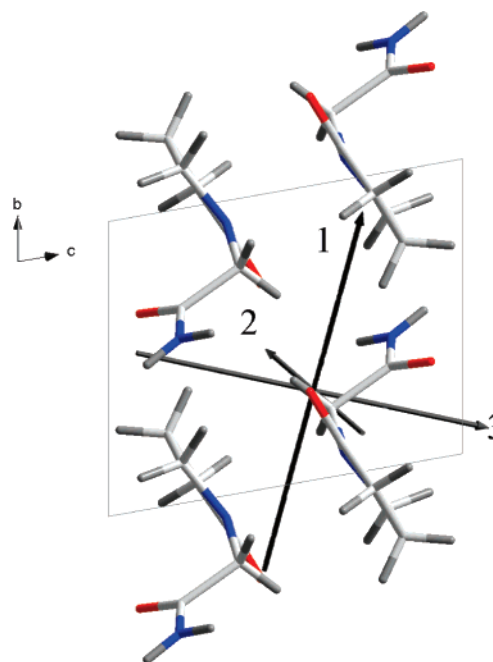

Figure 7. Directions of the principal axes of the strain ellipsoid in piracetam-V at 4.0 GPa viewed along the *a*-axis. Directions: 1, minimum compression; 2, medium compression; 3, maximum compression.

some degree of conformational flexibility. Such conformational flexibility is of course present in the piracetam molecule, and at ambient temperature there will be sufficient thermal energy available to overcome any conformational barriers. The structure of form V is very closely related to that of form II: the geometrical parameters of the molecules in the two forms are very similar, and the molecules are essentially superimposable, as shown in Figure 3. Figure 3 also shows an overlay of form II at 0.45 GPa and form V at 0.7 GPa and demonstrates how the phase transition involves a shearing of the unit cell. The most striking difference between the lattice parameters of the two forms is the increase of the β angle by ca. 10° associated with the II → V transition.

Phase transitions involving shearing of the unit cell are unusual but not unknown in organic crystals. For example, the monoclinic polymorph (form II) of the pigment Indigo is related to another monoclinic modification (form I) by a shear transition that is accompanied by an increase in the β angle of ca. 13°.[60] Another noteworthy example is represented by the hypnotic drug Zopiclone, in which the slipping of bilayer sheets by 6.61 Å along the *c*-axis and 1.48 Å along the *a*-axis facilitates the dehydration of the monoclinic dihydrate (form I) to the monoclinic anhydrate (form II).[61] Notable high-pressure phase transitions that involve a dramatic change in the β angle include that of sodium oxalate with a decrease in the β angle of 5° on going from 3.6 to 3.8 GPa[54,62] and of 1,3-cyclohexanedione with a change in the β angle of 4.17(2)° at pressures between 0.1 MPa and 0.3 GPa.[63]

The plots in Figures 4 and 5 illustrate the variation of unit-cell parameters, cell volume, and density with increasing pressure. Ambient-pressure values for form II were taken from the literature (CSD reference code BISMEV).[29] A discontinuity between 0.45 and 0.7 GPa is apparent in the plots of unit-cell axes and angles vs pressure. The discontinuity is less obvious in the plot of volume vs pressure, making ambiguous the assignment of this as a first- or second-order phase transition.
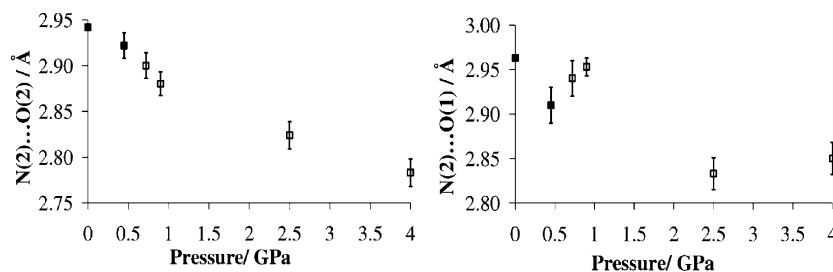
Figure 8. Variation of hydrogen-bonded D⋯A distances in form II and V as a function of pressure.
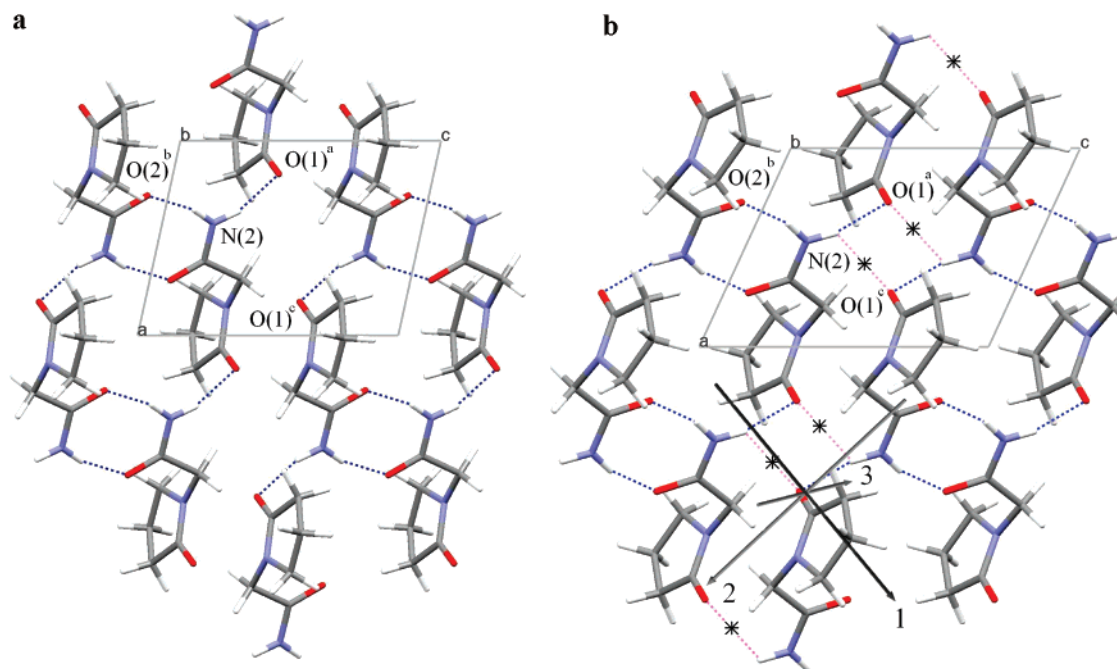
Figure 9. Crystal structures of (a) form II at ambient pressure and (b) form V at 4.0 GPa viewed along the *b*-axis. The new hydrogen bond present in form V and discussed in the main text is indicated by an asterisk. The directions of the principal axes of the strain ellipsoid in form V are also shown. The figures are drawn to the same scale. Symmetry codes: ^{a} −x, 1 − y, −1 − z; ^{b}1 − x, 1 − y, −z; ^{c}−x, −1 − y, −z.

Over the 0.7−4.0 GPa pressure range, the unit-cell volume decreased by ca. 19.6%. Rationalization of changes at the structural level as a function of pressure should be related to the linear strain in the directions of the principal axes of the strain ellipsoid rather than to the compressibilities of lattice parameters. This is because the unit cell is triclinic, and so none of the three strain tensor vectors is expected to lie along the unit-cell axes.

Strain tensor calculations were carried out using a locally written program,[64] based on the discussion in Hazen & Finger[65] and employing the JACOBI subroutine of Press et al.[66] Linear strain in the directions of the principal axes of strain ellipsoids vs pressure is shown in Figure 6.

The directions of the minimum, medium, and maximum compression with respect to the cell axes are shown in Figure 7: the same numbering scheme as in Figure 6 was used to differentiate between the three directions. The medium and maximum directions of compression correlate well with the directions of hydrogen bonding, while the minimum direction parallels the minimization of sterically unfavorable $CH_2⋯H_2C$ contacts.
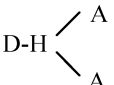
Comparison of Hydrogen-Bonded Patterns of Forms II and V. Since hydrogen atoms were placed geometrically and fixed during structure refinement, a discussion of hydrogen bonding should only be made on the basis of donor⋯acceptor (D⋯A) distances. On this basis, the assignment of the strength

of the hydrogen bonding has been made from the guideline values of strong, moderate, and weak hydrogen bonding as detailed by Jeffrey.[67]

Not surprisingly, the hydrogen-bond motifs of forms II and V are very similar, and both structures exhibit networks constructed of centrosymmetric hydrogen-bonded dimers of piracetam molecules, a motif commonly found in primary amides. For form II,[31] the descriptions of the hydrogen-bond pattern according to graph-set notation,[68] are a first-level graph set $N_1 = C(7)R_2^2(8)$ formed by cyclic dimerization of the two primary amide groups about the center of inversion, and a second-level graph set, $N_2 = R_4^4(18)$ that is a product of hydrogen-bond interaction between amide−amide and amide−pyrrolidone groups. The rings and chains form infinite ribbons connected by van der Waals interactions. Both hydrogen bonds are classified as "normal", i.e., two-atoms, according to Steiner.[69] Because of the large uncertainties associated with the D⋯A distances, only discussion of overall trends is possible. These are not significantly different within adjacent pressure measurements, but the D⋯A distances of both hydrogen bonds decrease over the 0.7−2.5 GPa pressure range (Table 3 and Figure 8).

The distance involved in the formation of the hydrogen-bonded centrosymmetric dimer [N(2)⋯O(2)] decreases by ca. 5.4% on going from form II at ambient pressure to form V at 4.0 GPa, and the distance involved in the hydrogen bond that

Table 3. D···A Distances for Atoms Involved in Normal and Bifurcated Hydrogen Bonds

D···A distance/ Å	Form II ambient pressure[a]	Form II 0.45 GPa	Form V 0.7 GPa	Form V 0.9 GPa	Form V 2.5 GPa	Form V 4.0 GPa
Normal D−H···A						
N(2)···O(2)[b]	2.942(2)	2.922(14)	2.900(14)	2.880(13)	2.824(15)	2.783(15)
N(2)···O(1)[c]	2.963(2)	2.91(2)	2.94(2)	2.953(10)	2.833(18)	2.850(18)
Bifurcated						
N(2)···O(1)[d]	4.022(2)[e]	3.916(13)[e]	3.389(16)	3.277(8)	3.064(15)	2.949(16)

[a] Ref 29. [b] Symmetry code: $-1 - x, -1 - y, -z$. [c] Symmetry code: $-1 + x, y, z$. [d] Symmetry code: $-x, -1 - y, 1 - z$. [e] Long contact.

links these dimers [N(2)···O(1)] decreases by ca. 3.8%. Although there are large standard uncertainties associated with this latter contact (see Table 3 and Figure 8), it does appear that it initially increases over the course of the phase transition; such an increase in a hydrogen-bond length associated with a pressure-induced phase transition is not an unknown phenomenon.[20,18,21] In particular, investigation of the crystal structure reveals that the geometry of the N(2)···O(1) hydrogen bond is susceptible to changes in the β angle, which increases by ca. 10° over the phase transition, and its direction is in fact parallel to the (1 0 1) planes in form V.

The transition to form V is associated with the formation of a new D···A contact involving N(2) and O(1) (see Table 3 and Figure 9). The distance of this contact is significantly reduced to 3.389(16) at 0.7 GPa Å [cf. 4.022(2) Å at ambient pressure for form II] and while still relatively long, it can now be classified as a weak hydrogen-bonding interaction. This results in the overall formation of a bifurcated hydrogen bond[69] from N(2)−H(9) (Figure 9) that satisfies the double-acceptor capability of the carbonyl oxygen, O(1). By 4.0 GPa, this intermolecular interaction is significantly shorter with a distance of ca. 2.95 Å. Assuming that geometrical placement of the hydrogen atoms belonging to the amide group is a relatively good approximation of true hydrogen-bonding geometry, and that no disorder is involved, a D−H···A angle of 107.2(4)° at 4.0 GPa makes this new hydrogen bond considerably weaker than the other [154.9(4)°]. At first sight, therefore, this contact seems unlikely to be the sole driving force for the transition, but careful inspection of the crystal structures shows no other structural changes or new contacts that might favor phase V. Thus, we are compelled to conclude that it is indeed the formation of this new interaction and the closure of structural voids that are the driving forces for the transformation. Similar driving forces for single-crystal to single-crystal pressure-induced phase transitions have also been observed by other authors for a variety of small organic molecules.[6,16−21,58]

Not surprisingly, the directions of hydrogen bonding correlate well with the directions of medium and maximum compression (Figure 9), thereby confirming the "soft" nature of this type of interaction, as noted by other authors.[6,15,20,21,42] In particular, the direction of maximum compression has a strong component along the direction of the bifurcated hydrogen bond, which, as noted above, is the one experiencing the most compression (Table 3).

The observation that form II transformed to form V on application of pressure while form IV transformed to form II on decompression[32] is particular intriguing and presumably reflects the fact that particular phases may be accessible only by certain pathways, i.e., a particular phase is formed only on decompression from a higher pressure phase. Such behavior is not uncommon in molecular crystals. For example, L-cysteine-

IV can be formed only by decompression of L-cysteine-III and not by compression of any of the other polymorphs of L-cysteine.[16] The high-pressure phase of CBr$_4$ is also only accessible on decompression,[70] as is the ζ form of glycine,[71] identified by Raman spectroscopy, and the orthorhombic form of paracetamol, although in the latter the transformation is not complete and poorly reproducible.[72]

For piracetam-II, it appears that the effect of increasing pressure is to lock the molecules into an arrangement where the interaction between the two primary amide groups dominates. While the conformational barriers between the molecules in forms II and IV are relatively low, the required change in molecular conformation would require the strong hydrogen bonding between the primary amide groups in form II to be disrupted, thus providing a substantial barrier to interconversion. At present, it is not possible to rule out that the single-crystal to single-crystal phase transition of form IV to form II on release of pressure might have occurred via a further transition to form V or that a transition from form V to form IV might occur at pressures higher than 4.0 GPa.

High-Pressure Crystallization from Solution: Piracetam Dihydrate. Initial attempts to induce crystallization from a 0.7 M aqueous solution proved unsuccessful up to a pressure of 1.0 GPa. Precipitation of polycrystalline material only occurred when the pressure was first raised to 1.6 GPa (inducing freezing of the aqueous solution to give ice-VI), followed by decrease of pressure to 0.6 GPa to give finely divided polycrystalline material. It was from this material that a single crystal (Figure 2) was grown at 0.6 GPa by careful temperature cycling as described in the experimental section. Indexing of the reflections obtained from a single-crystal X-ray diffraction experiment gave a triclinic unit cell with dimensions substantially different from any of the three known polymorphs of piracetam or of the recently discovered monohydrate.[32] Structure solution using direct methods with subsequent full-matrix least-squares structure refinement identified the crystal as a new dihydrate of piracetam.

Bond lengths and angles in piracetam dihydrate are similar to those found for the anhydrous polymorphs and for the monohydrate. The torsion angle of 118.0(5)° for C(6)−C(5)−N(1)−C(1) is similar to that found for the form IV of anhydrous piracetam, while the angle of 153.0(5)° for N(1)−C(5)−C(6)−N(2) is similar to that for forms II and III.

The crystal structure of the high-pressure dihydrate is characterized by a three-dimensional hydrogen-bonded network (Figure 10) that involves a total of six distinct hydrogen bonds. The three-dimensional network can be decomposed into a principal hydrogen-bonded chain motif that runs along the *a*-axis and is then translated along *b* (Figure 10a). The motif is extended along *c* by application of inversion symmetry (Figure 10b).
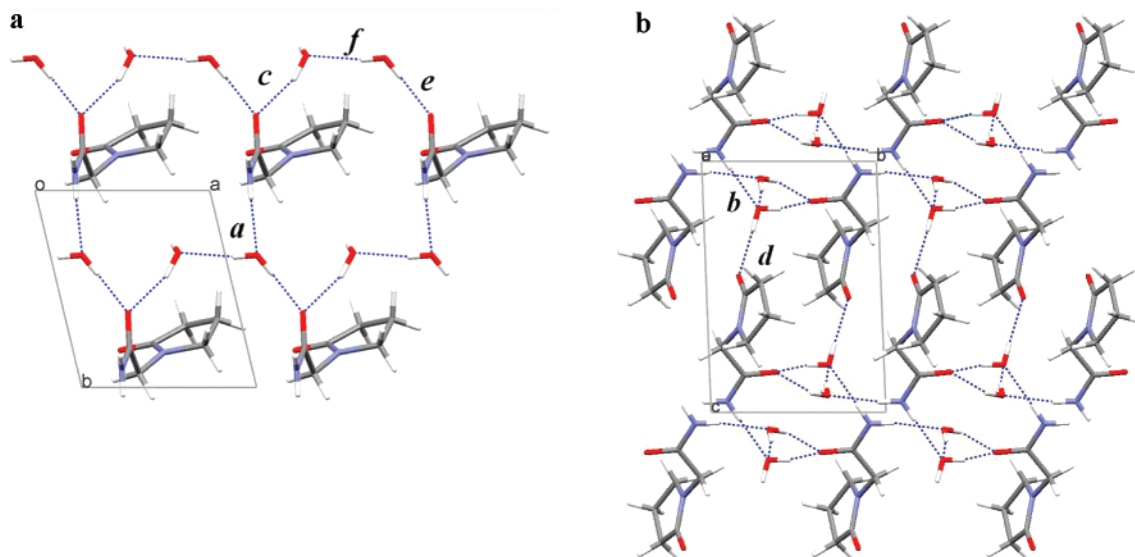
Figure 10. Hydrogen-bond motif of piracetam dihydrate viewed along the (a) *c* and (b) *a* crystallographic axes. Some layers have been omitted for clarity in (a). The labels refer to the types of hydrogen bonds described in Table 4.

Table 4. Hydrogen-Bonding Parameters in Piracetam Dihydrate

donor-H···acceptor/Å	hydrogen-bond label	D−H (Å)[a]	H···A (Å)	D···A (Å)	D−H···A (°)
N(2)−H(10)···O(12)[b]	a	1.01	1.91	2.922(4)	170(3)
N(2)−H(9)···O(11)[c]	b	1.01	1.92	2.921(3)	177(6)
O(11)−H(111)···O(2)	c	0.98	1.86	2.788(6)	158(5)
O(11)−H(112)···O(1)[d]	d	0.98	1.79	2.762(3)	171(7)
O(12)−H(121)···O(2)	e	0.98	1.95	2.902(4)	163(4)
O(12)−H(122)···O(11)[e]	f	0.98	1.82	2.788(8)	168(6)

[a] The distances to hydrogen have been normalized with the program *PLATON*[72] to mimic those that might be obtained by neutron diffraction. [b] Symmetry code: x, 1 + y, z. [c] Symmetry code: −x, −y, −z. [d] Symmetry code: −x, −y, 1 − z. [e] Symmetry code: −1 + x, y, z.

In contrast to piracetam monohydrate, no dimers or other hydrogen-bonded contacts are found between piracetam molecules, which are instead linked via hydrogen bonds to and from water molecules. Within the piracetam molecules, the nitrogen atom of the primary amide, N(2), donates two hydrogen bonds to two crystallographically independent water oxygen atoms. The oxygen atom of the primary amide, O(2), fulfills its double acceptor capability, accepting two hydrogen bonds from two crystallographically independent water molecules, while the oxygen atom of the tertiary amide O(1) accepts only one hydrogen bond. One water oxygen atom, O(11), fulfills its double acceptor capability through involvement in a further hydrogen bond from a crystallographically distinct water molecule. This scheme, along with hydrogen-bonding parameters, is summarized in Table 4, with the atom labeling depicted in Figure 11.

According to the classification of the strength of hydrogen-bonding based on geometrical parameters by Jeffrey,[67] all six hydrogen bonds are of "medium" strength, with values for the D−H···A angle approaching linearity.

Combination of the six hydrogen bonds gives overall first-level and second-level graph sets for piracetam dihydrate $N_1 = $ DDDD and $N_2 = D_2^2(5)D_2^2(6)R_4^4(12)D_2^2(9)$ $C_2^2(9)R_4^4(18)C_2^2$-$(6)D_2^2(6)D_2^1(3)D_2^2(6)D_2^2(4)D_2^1(3)D_2^2(4)D_2^2(4)D_2^2(5)$, respectively. These were confirmed using the GSET routine in *RPLUTO*.[74] A matrix representation of these graph sets is given in Supporting Information.

Stability of Piracetam Dihydrate. To investigate the stability of piracetam dihydrate toward pressure and temperature, a series
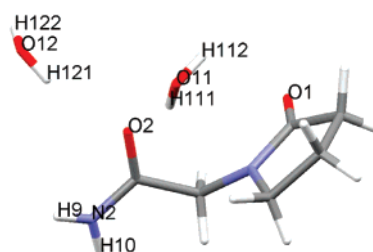

Figure 11. Atom labeling for the hydrogen-bond scheme in Table 4.

of additional experiments were performed. First, the pressure inside the DAC was increased from 0.6 to 1.0 GPa. The single crystal remained intact and was identified by single-crystal X-ray diffraction as the dihydrate but with a ca. 4.3% increase in density with respect to the structure at 0.6 GPa. The pressure inside the cell was then increased to ca. 1.3 GPa, and again the crystal remained intact. On heating the cell to ca. 323 K, the single crystal of the dihydrate was observed to dissolve, and new block-like crystallites simultaneously grew from the edge of the gasket. The appearance of these new crystallites was in marked contrast to the finely divided powder from which the dihydrate was first grown at 0.6 GPa. Unfortunately, all crystallites were accidentally dissolved while we were attempting to grow a single crystal at 1.3 GPa. However, it proved possible to crystallize morphologically similar, block-like crystallites by lowering the pressure inside the gasket, and in this way single crystals were successfully grown at ca. 0.7 and 0.4 GPa in two separate experiments. X-ray diffraction revealed these to be anhydrous form IV. Given the reasonable assumption that the block-like crystals that appeared on heating the dihydrate at 1.3 GPa were also in fact form IV, it is postulated that the dihydrate transformed to form IV by dehydration as a response to heating at high pressure. A possible mechanism for this dehydration might involve the breaking of the hydrogen-bonded network and cooperative rotation of piracetam molecules to form the dimers observed in form IV. Support for such a mechanism is provided by comparison of the two structures. Both structures contain neighboring molecules that lie at similar separations, as illustrated in Figure 12. The torsion angle C(6)−C(5)−N(1)−C(1) is quite similar for the dihydrate and form IV [118.0(5)° and 115.4(7)°, respectively] and so the main rotation would be
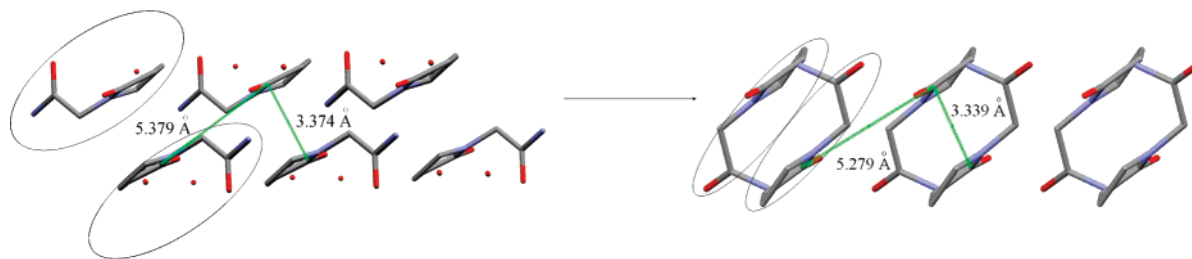
Figure 12. A potential mechanism for the dehydration of the dihydrate of piracetam to anhydrous form IV involving the collapse of the hydrogen-bonded network and the cooperative rotation of molecules. The values refer to distances between C(1) atoms of neighboring molecules. Circled molecules are involved in dimer formation by cooperative rotation.

Scheme 1.   Transformations of Polymorphs and Hydrates of Piracetam
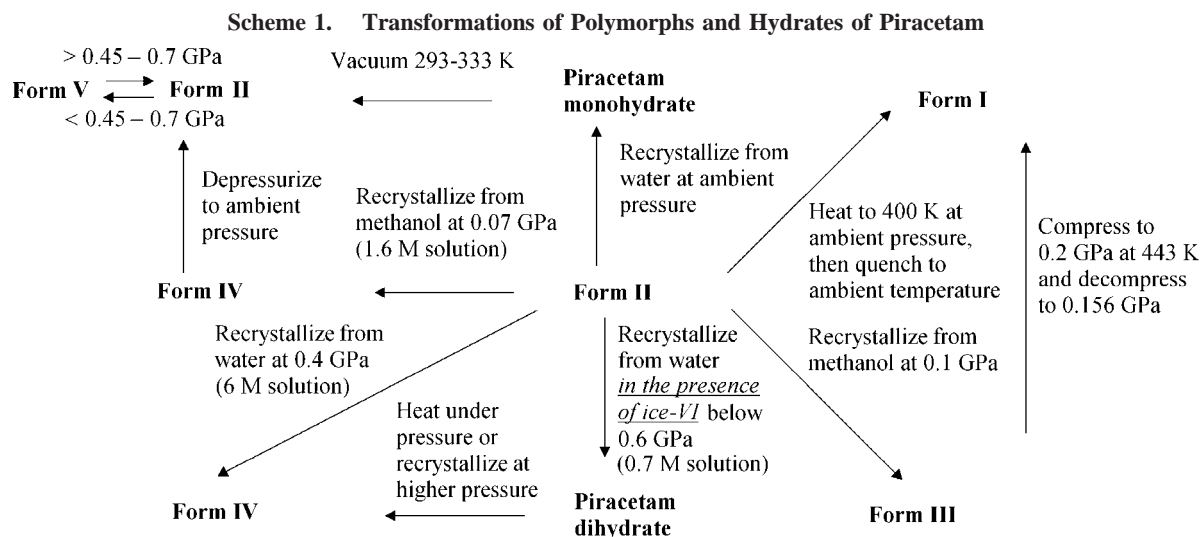
about the N(1)−C(5)−C(6)−N(2) torsion angle [153.0(5)° and 32.0(7)°, respectively].

These results also shed light on how piracetam dihydrate crystallized in the first instance and illustrate a novel and interesting strategy for the preparation of hydrates at high pressure. Compression of liquid water at ambient temperature leads to the formation of tetragonal ice-VI at pressures greater that 1.05 GPa[75] and to cubic ice-VII above 2.1 GPa.[76] Hence, at 1.6 GPa the aqueous solution of piracetam froze to give polycrystalline ice-VI. Not only would this have provided numerous nucleation sites, but it would also substantially increase the concentration of piracetam in solution−both factors encouraging crystallization. Furthermore, crystallization in the presence of ice might also be expected to encourage the formation of hydrates−examples of this phenomenon have been observed at ambient pressure when solutions of aqueous paracetamol were flash cooled to 273 K to give paracetamol trihydrate.[77]

Conclusions

The transformations between the polymorphs and hydrates of piracetam observed in this and other work are summarized in Scheme 1.

It is clear from the results of this study that recrystallization of aqueous solutions of piracetam under a range of conditions (pressure, concentration, temperature) allows one to select which polymorph or hydrate is produced and provides insight into how these polymorphs and hydrates interconvert. The technique can therefore be regarded as an additional tool for crystal engineering. In particular, the use of pressure provides an additional, useful dimension for the exploration of polymorphism and solvate formation in pharmaceutical compounds.

Perhaps the most significant result is the observation that crystallization in the presence of high-pressure ice-VI allows access to a new dihydrate. This result, in combination with the observation that crystallization in the presence of ice-I*h* at ambient pressure can give hydrates of paracetamol,[77] points to a new line of research that would involve crystallization of materials by first inducing crystallization of different forms of ice (e.g., I*h*, II, V, VI, and VII) depending on pressure and temperature. These different forms of ice may subsequently induce the precipitation of different polymorphs or hydrates of the material under study. In principle, this strategy should also be applicable to the preparation of other solvates through pressure-induced freezing of the solvent. So far, attempts to recover piracetam-IV and piracetam dihydrate to ambient pressure have not been successful; piracetam-IV transforms to piracetam-II, and piracetam dihydrate appears to dissolve when the pressure is released. However, there may be scope for recovering these materials at low temperature or by rapid removal of excess solvent to prevent dissolution or solvent-mediated phase transformations.

Supporting Information Available: Crystallographic information files (CIFs) and hydrogen-bonding graph-set assignments for piracetam dihydrate are available free of charge via the Internet at http://pubs.acs.org.

References

(1) Bernstein, J. In *Polymorphism in Molecular Crystals*, IUCr Monographs on Crystallography; Clarendon Press: Oxford, 2002.

(2) Yu, L.; Reutzel, S. M.; Stephenson, G. A. *Pharm. Sci. Technol. Today* **1998**, *1*, 118−127.

(3) Vippagunta, S. R.; Brittain, H. G.; Grant, D. J. W. *Adv. Drug Delivery Rev.* **2001**, *48*, 3−26.

(4) *Chem. Eng. News* **2003**, (February) *81*, 32−35.

(5) Tozuka, Y.; Kawada, D.; Oguchi, T.; Yamamoto, K. *Int. J. Pharm.* **2003**, *263*, 45−50.

(6) Boldyreva, E. V. In *High Pressure Crystallography*; Katrusiak, A., McMillan, P. F., Eds.; NATO Science Series II Mathematics, Physics & Chemistry; Kluwer: Dordrecht, 2004; pp 495−512, and references therein.

(7) Fabbiani, F. P. A.; Pulham, C. R. *Chem. Soc Rev.* **2006**, *35*, 932−942, and references therein.

(8) Boldyrev, V. V. *J. Mater. Sci.* **2004**, *39*, 5117−5120, and references therein.

(9) Bridgman, P. W. In *The Physics of High Pressure*; G. Bell and Sons: London, 1931.

(10) Bridgman, P. W. In *Collected Experimental Papers*; Harvard University Press: Cambridge, Massachussetts, 1964.

(11) Okumura, T.; Ishida, M.; Takayama, K.; Otsuka, M. *J. Pharm. Sci.* **2006**, *95*, 689−700.

(12) Boldyreva, E. V.; Ahsbahs, H.; Uchtmann, H.; Kascheeva, N. E. *High Press. Res.* **2000**, *17*, 79−99.

(13) Boldyreva, E. V. *J. Mol. Struct.* **2003**, *647*, 159−179, and references therein.

(14) Boldyreva, E. V.; Dmitriev, V.; Hancock, B. C. *Int. J. Pharm.* **2006**, *327*, 51−57.

(15) McGregor, P. A.; Clark, S. J.; Allan, D. R.; Parsons, S. *Acta Crystallogr.* **2006**, *B62*, 599−605, and references therein.

(16) Moggach, S. A.; Allan, D. R.; Clark, S. J.; Gutmann, M. J.; Parsons, S.; Pulham, C. R.; Sawyer, L. *Acta Crystallogr.* **2006**, *B62*, 296−309, and references therein.

(17) Boldyreva, E. V.; Ivashevskaya, S. N.; Sowa, H.; Ahsbahs, H; Weber, H-P *Z. Kristallogr.* **2005**, *220*, 50−57, and references therein.

(18) Katrusiak, A. *Cryst. Res. Technol.* **1991**, *26*, 523−531, and references therein.

(19) Hemley, R. J.; Dera, P.; *Rev. Min. Geochem.* **2000**, *41*, 335−419.

(20) Boldyreva, E. V. *J. Mol. Struct.* **2004**, *700*, 151−155.

(21) Katrusiak, A. In *High Pressure Crystallography*; Katrusiak, A., McMillan, P. F., Eds.; NATO Science Series II Mathematics, Physics & Chemistry; Kluwer: Dordrecht, 2004; pp 513−520, and references therein.

(22) Fourme, R. *J. Appl. Cryst.* **1968**, *1*, 23−30.

(23) Gajda, R.; Dziubek, K.; Katrusiak, A. *Acta Crystallogr.* **2006**, *B62*, 86−93, and references therein.

(24) Gajda, R.; Katrusiak, A. *Acta Crystallogr.* **2007**, *B63*, 111−117, and references therein.

(25) Fabbiani, F. P. A.; Allan, D. R.; David, W. I. F.; Moggach, S. A.; Parsons, S.; Pulham, C. R. *CrystEngComm* **2004**, *6*, 504−511.

(26) Fabbiani, F. P. A.; Allan, D. R.; Parsons, S.; Pulham, C. R. *Acta Crystallogr.* **2006**, *B62*, 826−842.

(27) Fabbiani, F. P. A.; Allan, D. R.; Marshall, W. G.; Parsons, S.; Pulham, C. R.; Smith, R. I. *J. Cryst. Growth* **2005**, *275*, 185−192.

(28) Fabbiani, F. P. A.; Allan, D. R.; Dawson, A. D.; David, W. I. F.; McGregor, P. A.; Oswald, I. D. H.; Parsons, S.; Pulham, C. R. *Chem. Commun.* **2003**, 3004−3005.

(29) Bandoli, G.; Clemente, D. A.; Grassi, A.; Pappalardo, G. C. *Mol. Pharmcol.* **1981**, *20*, 558−564.

(30) Admiraal, G.; Eikelenboom, J. C.; Vos, A. *Acta Crystallogr.* **1982**, *B38*, 2600−2605.

(31) Louër, D.; Louër, M.; Dzyabchenko, V. A.; Agafonov, V.; Céolin, R. *Acta Crystallogr.* **1995**, *B51*, 182−187.

(32) Fabbiani, F. P. A.; Allan, D. R.; Parsons, S.; Pulham, C. R. *CrystEngComm* **2005**, *7*, 179−186.

(33) Toscani, S. *Thermochim. Acta* **1998**, *321*, 73−79.

(34) Kühnert-Brandstätter, M.; Bürger, A.; Völlenkee, R. *Sci. Pharm.* **1994**, *62*, 307−316.

(35) Céolin, R.; Agafonov, R.; V.; Louër, D.; Dzyabchenko, V. A.; Toscani, S.; Cense, J. M. *J. Sol. State Chem.* **1996**, *122*, 186−194.

(36) Ter Minassian, L.; Milliou, F. *J. Therm. Anal.* **1992**, *38*, 181−196.

(37) Pertsin, A. J.; Kitaigorodskii, A. I. In *The Atom-Atom Potential Method*; Springer: Berlin, 1987.

(38) Nowell, H.; Price, S. L. *Acta Crystallogr.* **2005**, *B61*, 558−568.

(39) Vishweshwar, P.; McMahon, J. A.; Peterson, M. L.; Hickey, M. B.; Shattocka, T. R.; Zaworotko, M. J. *Chem. Commun.* **2005**, 4601−4603.

(40) Merrill, L.; Bassett, W. A. *Rev. Sci. Instrum.* **1944**, *45*, 290−294.

(41) Piermarini, G. J.; Block, S.; Barnett, J. D.; Forman, R. A. *J. Appl. Phys.* **1975**, *46*, 2774−2780.

(42) Moggach, S. A.; Allan, D. R.; Parsons, S.; Sawyer, L.; Warren, J. E. *J. Synchrotron Rad.* **2005**, *12*, 598−607.

(43) Dawson, A.; Allan, D. R.; Parsons, S.; Ruf, M. *J. Appl. Crystallogr.* **2004**, *37*, 410−416.

(44) Bruker AXS, *SAINT*, Version 7.01A; Bruker-AXS: Madison, Wisconsin, U.S.A., 2003.

(45) Parsons, S. *SHADE*; The University of Edinburgh: Scotland, 2004.

(46) Sheldrick, G. M.; *SADABS*, version 2004/1; University of Göttingen: Germany, 2004.

(47) Blessing, R. H. *Acta Crystallogr.* **1995**, *B51*, 33−38.

(48) Farrugia, L. J. *J. Appl. Cryst.* **1999**, *32*, 837−838.

(49) Altomare, A.; Cascarano, A.; G.; Giacovazzo, C.; Guagliardi, A.; *J. Appl. Cryst.* **1993**, *26*, 343−350.

(50) Betteridge, P. W.; Carruthers, J. R.; Cooper, R. I.; Prout, C. K.; Watkin, D. J. *J. Appl. Cryst.* **2003**, *36*, 1487.

(51) Bruno, I. J.; Cole, J. C.; Edgington, P. R.; Kessler, M.; Macrae, C. F.; McCabe, P.; Pearson, J.; Taylor, R. *Acta Crystallogr.* **2002**, *B58*, 389−397.

(52) Crystal Impact, DIAMOND, Version 3.0; Crystal Impact GbR: Bonn, Germany, 2004.

(53) Goryainov, S. V.; Kolesnik, E. N.: Boldyreva, E. V. *Phys. B Condens. Matt.* **2005**, *357*, 340−347.

(54) Boldyreva, E. V.; Ahsbahs, H.: Chernyshev, V. V.; Ivashevskaya, S. N.; Oganov, A. R. *Zeit. Krist.* **2006**, *221*, 186−197.

(55) Boldyreva, E. V.; Sowa, H.; Seryotkin, Yu. V.; Drebushchak, T. N.; Ahsbahs, H.; Chernyshev, V. V.; Dmitriev, V. P. *Chem. Phys. Lett.* **2006**, *429*, 474−478.

(56) Drebushchak, T. N.; Sowa, H.; Seryotkin, Yu. V.; Boldyreva, E. V.; Ahsbahs, H. *Acta Crystallogr.* **2006**, *E62*, o4052−o4054.

(57) Dawson, A.; Allan, D. R.; Belmonte, S. A.; Clark, S. J.; David, W. I. F.; McGregor, P. A.; Parsons, S.; Pulham, C. R.; Sawyer, L. *Cryst. Growth Des.* **2005**, *5*, 1415−1427.

(58) Moggach, S. A.; Allan, D. R; Morrison, C. A.; Parsons, S.; Sawyer, L. *Acta Crystallogr.* **2005**, *B61*, 58−68.

(59) Wood, P. A.; Forgan, R. S.; Henderson, D.; Parsons, S.; Pidcock, E.; Tasker, P. A.; Warren, J. E. *Acta Crystallogr.* **2006**, *B62*, 1099−1111.

(60) Eller-Pandraud, H. *Bull. Soc. Chim. Fr.* **1958**, 316−317.

(61) Shankland, N.; David, W. I .F.; Shankland, K.; Kennedy, A. R.; Frampton, C. S.; Florence, A. J. *Chem. Commun.* **2001**, 2204−2205.

(62) Goryainov, S. V.; Boldyreva, E. V.; Smirnov, M. B.; Ahsbahs, H.; Chernyshev, V. V.; Weber, H.-P. *Dokl. Phys. Chem.* **2003**, *390*, 154−157.

(63) Katrusiak, A. *Acta Crystallogr.* **1990**, *B46*, 246−256.

(64) Parsons, S. *STRAIN*; The University of Edinburgh: Scotland, 2005.

(65) Hazen, R. M.; Finger, L. W. In *Comparative Crystal Chemistry*; John Wiley and Sons: Chichester, 1982; p 81.

(66) Press, W. H.; Teukolsky, S. A; Vetterling, W. T.; Flannery, B. P. In *Numerical Recipes in Fortran*, 2nd ed.; Cambridge University Press: Cambridge, 1992.

(67) Jeffrey, G. A. In *An Introduction to Hydrogen Bonding*; Oxford Universty Press: Oxford, 1997.

(68) Etter, M. C. *Acc. Chem. Res.* **1990**, *23*, 120−126. Etter, M. C.; MacDonald, J. C.; Bernstein, J. *Acta Crystallogr.* **1990**, *B46*, 256−262.

(69) Steiner, T. *Angew. Chem., Int. Ed.* **2000**, *41*, 48−76.

(70) Bridgman, P. W. *Rev. Mod. Phys.* **1946**, *18*, 1−93.

(71) Goryainov, S. V.; Boldyreva, E. V.; Kolesnik, E. N. *Chem. Phys. Lett.* **2006**, *419*, 496−500.

(72) Boldyreva, E. V.; Shakhtshneider, T. P.; Ahsbahs, H.; Sowa, H.; Uchtmann, H. *J. Therm Anal. Calorim.* **2002**, *66*, 437−452.

(73) Spek, A. L. *PLATON*; University of Utrecht: The Netherlands, 2000.

(74) Motherwell, W. D. S.; Shields, G. P.; Allen, F. H. *Acta Crystallogr.* **1999**, *B55*, 1044−1056.

(75) Kamb, B. *Science* **1965**, *150*, 205−209.

(76) Kamb, B.; Davis, B. L. *Proc. Natl. Acad. Sci. U.S.A.* **1964**, *52*, 1433−1439.

(77) McGregor, P. A.; Allan, D. R.; Parsons, S.; Pulham, C. R. *J. Pharm. Sci.* **2002**, *91*, 1308−1311.